Progressive loss of epidermal growth factor receptor in a subpopulation of breast cancers: implications in target-directed therapeutics

Lee-Yee Choong,[1] Simin Lim,[1] Marie Chiew-Shia Loh,[6] Xiaohui Man,[1] Yunhao Chen,[1] Weiyi Toy,[1] Mengfei Pan,[1] Chien-Shing Chen,[1] Anuradha Poonepalli,[2] M. Prakash Hande,[2] Puay-Hoon Tan,[4] Manuel Salto-Tellez,[1] Chow-Yin Wong,[5] Nilesh Shah,[1] Brian J. Druker,[7] and Yoon-Pin Lim[1,3,6]

[1]Oncology Research Institute, [2]Department of Physiology, Yong Loo Lin School of Medicine, and [3]Department of Biological Sciences, Faculty of Science, National University of Singapore; Departments of [4]Pathology and [5]General Surgery, Singapore General Hospital; [6]Bioinformatics Institute, Agency for Science, Technology, and Research, Singapore; and [7]Howard Hughes Medical Institute, Oregon Health & Science University, Portland, Oregon

Abstract

Understanding the molecular etiology and heterogeneity of disease has a direct effect on cancer therapeutics. To identify novel molecular changes associated with breast cancer progression, we conducted phosphoproteomics of the MCF10AT model comprising isogenic, ErbB2- and ErbB3-positive, xenograft-derived cell lines that mimic different stages of breast cancer. Using *in vitro* animal model and clinical breast samples, our study revealed a marked reduction of epidermal growth factor receptor (EGFR) expression with breast cancer progression. Such diminution of EGFR expression was associated with increased resistance to Gefitinib/Iressa *in vitro*. Fluorescence *in situ* hybridization showed that loss of *EGFR* gene copy number was one of the key mechanisms behind the low/null expression of EGFR in clinical breast tumors. Statistical analysis on the immunohistochemistry data of EGFR expression from 93 matched normal and breast tumor samples showed that (*a*) diminished EGFR expression could be detected as early as in the preneoplastic lesion (ductal carcinoma *in situ*) and this culminated in invasive carcinomas; (*b*) EGFR expression levels could distinguish between normal tissue versus carcinoma *in situ* and invasive carcinoma with high statistical significance ($P < 0.001$, $n = 81$). However, no significant correlation of EGFR expression with disease-free survival and overall survival was observed. This is the first time EGFR expression has been tracked meaningfully and developmentally from the normal condition through disease progression using *in vitro*, xenograft, and matched normal and tumor samples. Thus, our study provides a new insight into the role of EGFR in breast cancer development. Although no value of EGFR expression in prognosis was found, our findings are likely to have implications in the design of clinical trials targeting the EGFR family of proteins in breast cancer. [Mol Cancer Ther 2007;6(11):2828–42]

Introduction

There are ~518 putative protein kinase genes identified in the human genome (1). About 100 of these are tyrosine kinases and the rest are serine/threonine kinases (2). Many kinases have been implicated in various human malignancies (3) and they represent attractive biomarkers and drug targets (4). It is a widely accepted notion that overexpression of tyrosine kinases such as ErbB2 and Src contributes to breast oncogenesis (5). However, the function of epidermal growth factor receptor (EGFR) in breast cancer is not as clear. Although the overexpression of EGFR has been linked to a more aggressive breast tumor phenotype and poorer prognosis (6, 7), some have reported otherwise (8, 9). There is a need for a greater understanding of the role of EGFR during breast cancer development. Trials involving target-directed therapeutics have been ineffective because of the poor understanding of the molecular etiology of disease and the epidemiology of drug targets. One excellent example is that of Gefitinib and non–small cell lung cancer. After years of disappointing clinical trial results, we now know that response to Gefitinib correlates well with *EGFR* mutation, which occurs at high frequency in people who are of Asian origin, women, nonsmokers, and those diagnosed with adenocarcinomas (10). Analogous to the early experience with Gefitinib and non–small cell lung cancer, most clinical trials involving the use of EGFR inhibitors and breast cancer were not promising and the reasons are poorly understood (11). Hence, studying the etiologic molecular changes associated with breast cancer progression is of strategic significance in managing this disease.

Received 12/29/06; revised 7/18/07; accepted 9/14/07.

Grant support: Biomedical Research Council, Agency for Science, Technology and Research, and the Office of Life Sciences, National University of Singapore.

The costs of publication of this article were defrayed in part by the payment of page charges. This article must therefore be hereby marked *advertisement* in accordance with 18 U.S.C. Section 1734 solely to indicate this fact.

Requests for reprints: Yoon-Pin Lim, Oncology Research Institute, National University of Singapore, Centre for Life Sciences, 28 Medical Drive, 02-14C, Singapore 117456. Phone: 65-6516-1313; Fax: 65-6873-9664. E-mail: nmilyp@nus.edu.sg

doi:10.1158/1535-7163.MCT-06-0809

Although clinical samples are valuable resources for understanding breast tumor biology, it is not an ideal minefield for biomarker discovery because normal breast tissues frequently have high contents of fat and low numbers of epithelial cells which impede global protein analysis used in comparative studies of tumor samples. To resolve these issues, we adopted the xenograft-derived MCF10AT model comprising isogenic derivatives of the MCF10A mammary epithelial cell line that represents different stages of breast cancer progression (12, 13). The MCF10AT cells were derived from MCF10A normal mammary epithelial cells transfected with T24 constitutively active RAS mutant. Although *RAS* mutations are rare in breast cancer, it is commonly activated in breast cancer by overexpressed growth factor receptors, which signal through RAS (14). Hence, this model is likely to reflect a subset of human breast cancers and their progression. Indeed, the MCF10AT model has several salient features of proliferative breast disease in humans including (*a*) the histologic spectrum of lesions (e.g., hyperplasia and carcinoma *in situ*); (*b*) the presentation of a mixture of these lesions in a single host, i.e., disease heterogeneity; (*c*) the production of invasive malignancy with some frequency, and (*d*) the progression of disease over a time range that is compatible with those observed during the highly sporadic nature of cancer development in humans. Consequently, it has been characterized by various groups in the areas of cytogenetics, apoptosis, transforming growth factor-β signaling, and protein expression (15–21). Whereas expression studies via cDNA microarray and proteomics have been useful in many instances, phosphoproteomics permits the focus on signaling proteins regulated by phosphorylation/dephosphorylation events. For this reason, we have previously developed methodologies that allow us to globally profile the tyrosine phosphorylation status of proteins in different biological conditions (22–24). Applying these tools to the MCF10AT model, we identified the progressive loss of EGFR expression during breast cancer development in this study. Validation of EGFR expression in clinical samples, investigation of the mechanism underlying the loss of EGFR in breast cancer, and the clinical significance of these data will be discussed.

Materials and Methods

Reagents

Gefitinib (IRESSA/ZD1839) was a kind gift from AstraZeneca. Peroxidase-conjugated phosphotyrosine antibodies (PY20-HRPO), anti-EGFR (COOH terminus), anti-ErbB2, anti-RAS, anti-ERK1, and anti–phosphoinositide-3-kinase (PI3K) p110α antibodies (for immunoblotting) were purchased from Transduction Laboratories. Anti-PI3K p110α antibody (for immunoprecipitation) was purchased from Upstate Biotechnology, Inc. Anti-AKT (5G3, for immunoprecipitation), anti-AKT (for immunoblotting), anti–phospho-AKT (Ser^{473}), anti–phospho-p44/42 mitogen-activated protein kinase (MAPK; Thr^{202}/Tyr^{204}), anti–phospho-mTOR (Ser^{2448}; 49F9), anti-S6 ribosomal protein (54D2), anti–phospho-S6 ribosomal protein ($Ser^{235/236}$), and anti–phospho-S6 ribosomal protein ($Ser^{240/244}$) were purchased from Cell Signaling Technology. Anti-mTOR antibodies were from Zymed. Anti-p70S6 kinase antibody (BL 704) antibody was from Bethyl Laboratories, Inc. Anti–phospho-p70 S6 kinase (pT421/pS424) rabbit monoclonal antibody was from Epitomics, Inc. Anti-EGFR (NH_2 terminus) and anti-ER antibodies for immunohistochemistry, modified antigen retrieval kit (citrate buffer; pH 6), polymer-HRP–conjugated anti-mouse IgG secondary antibodies, and diaminobenzidine were from Dakocytomation.

Cell Culture, Protein Sample Preparation, and Analysis

Xenograft-derived breast cancer cell lines (MCF10A1, MCF10AT1KCl.2, MCF10CA1h, and MCF10CA1aCl.1) were obtained from Dr. Fred Miller at the Barbara Ann Karmanos Cancer Institute, Detroit, MI. Cells were cultured as previously described elsewhere (20). Cells were incubated at 37°C in a humidified atmosphere containing 5% CO_2 and were routinely serum-starved for 16 h before stimulation with 50 ng/mL of epidermal growth factor (EGF) for the indicated periods of time. For protein extraction, cells grown in 150-mm tissue culture dishes were rinsed with ice-cold PBS before lysis in 1 mL of nondenaturing buffer [50 mmol/L Tris-HCl (pH 7.5), 0.5% Triton X-100, 0.5% Igepal, 150 mmol/L NaCl, 1 mmol/L EDTA, 50 mmol/L NaF, 1 mmol/L Na_3VO_4 plus protease inhibitors]. Protein lysates were clarified by centrifugation at 4°C using an Eppendorf microcentrifuge at 14,000 rpm for 10 min. Estimation of protein concentration was done using a bicinchoninic acid assay kit (Pierce Biotechnology). Immunoblotting and immunoprecipitation were done as per previous reports (23, 25).

Phosphoproteomics

Serum-starved cells were treated with 1 mmol/L of pervanadate for 15 min and lysed. 4G10-based immunoaffinity purification was similarly done as previously reported except that the enriched phosphoproteins were eluted with a buffer that was PBS-based rather than Tris-based (23). Sixty milligrams of total protein from each cell line was used for purification, and the enriched phosphoprotein contents of four samples were determined. These phosphoproteins were then denatured and the cysteines blocked as described in the isobaric tagging for relative and absolute quantification (iTRAQ) protocol (Applied Biosystems). Each sample was then digested with trypsin provided in the reagent kit at 37°C overnight (16 h) and labeled with the iTRAQ tags as follows: A1 (114 tag), 1k (115 tag), 1h (116 tag) and 1a (117 tag). To ensure complete labeling and avoid possible quantification errors resulting from different numbers of isotopes in the reagents, each sample was treated with two vials of the same labeling reagent. The labeled samples were then pooled and cleaned-up by the cation exchange cartridge provided in the reagent kit. The sample was desalted, lyophilized, and analyzed using electrospray ionization-liquid chromatography tandem mass spectrometry.

Online electrospray ionization-liquid chromatography tandem mass spectrometry was done using a QSTAR-XL

hybrid quadrupole-time of flight tandem mass spectrometer (Applied Biosystems) coupled to an LC-Packings (Dionex) liquid chromatography system comprising of a FAMOS autoinjector unit, a SWITCHOS 10-port valve unit, and an ULTIMATE^{PLUS} nano-flow pumping unit. The sample was injected into a reversed-phase C-18 peptide–trapping cartridge (300 μm × 5 mm; LC-Packings) in a flow of 0.1% formic acid for 5 min at 25 μL/min. Following the wash step, the flow from the ULTIMATE^{PLUS} was diverted back through the trapping cartridge at 100 nL/min using the SWITCHOS. Peptides were eluted from the cartridge by application of a gradient from 0% to 90% of acetonitrile in 0.1% formic acid over 40 min at 100 nL/min, and separated by passing through a column which was packed in-house and comprised of a 75 μm × 10 cm packed volume of 5 μm C-18 reversed phase packing (Column Engineering). Peptides eluting from the column were sprayed directly into the orifice of the mass spectrometer, which was run in information-dependent acquisition mode selecting all 2^+ to 4^+ charged ions with signal intensity greater than eight counts per second over the mass range of 300 to 2,000 amu. For collision-induced dissociation, nitrogen gas was used at a setting of 4 and the collision energy set to automatic, allowing increased energy with increasing ion mass. Each fraction aliquot that was run was searched against the human subset of the IPI protein database (EBI) using the MASCOT (Matrix Science) search engine. From the search results, a mass exclusion list was generated for each fraction based on the peptide masses of all matching peptides or up to a maximum of 2,000 masses. These masses were then excluded from tandem mass spectrometry fragmentation when the remaining aliquot of each fraction was rerun. For protein identification and quantification, the complete set of data files (*.wiff) was analyzed together using ProteinPilot software 1.0 revision number 33087 (Applied Biosystems) and searched against the human subset of the UniProt protein database (v6.7, 71070 sequences; EBI) using the Paragon algorithm. The search was restricted to tryptic peptides. Cysteine methanethiolation, NH_2-terminal iTRAQ labeling, iTRAQ-labeled lysine, serine, threonine and tyrosine phosphorylation, and methionine oxidation were selected as variable modifications. One missing cleavage was allowed. Precursor error tolerance was set to 200 ppm and tandem mass spectrometry fragment error tolerance to 0.5 Da. Unused (conf) cutoff was set to 1.3 to achieve 95% confidence.

Xenografts, Clinical Samples, and Immunohistochemistry

The protocol for the *in vivo* study was reviewed and approved by the Institutional Animal Care and Use Committee of the National University of Singapore in compliance with international guidelines on the care and use of animals for scientific purposes. A1 (10^7), 1k (5×10^6), 1h (10^6), and 1a (3×10^5) cells in a PBS and Matrigel (BD Biosciences) mixture (1:1) were injected s.c. into severe combined immunodeficiency mice at three different sites (front and back flanks) and observed weekly. Matched malignant and adjacent normal breast tissues were requested from the tissue repositories of the National Cancer Centre of Singapore and National University Hospital following approval from the institutional review boards of the National Cancer Centre of Singapore, National University Hospital, and the National University of Singapore. Histopathology reports were also obtained along with the samples.

Frozen tissues from xenografts were freshly prepared for immunohistochemistry by fixing them in 10% neutral buffered formalin (Sigma) for 16 h at 4°C, subject to ThermoShandon tissue processor and embedded in paraffin. Sections were warmed in a 60°C oven and dewaxed in three changes of xylene and passaged through graded alcohols. For EGFR, pAKT, and pERK, antigen retrieval was done using the Target Retrieval Solution (Dakocytomation) at 95°C for 40 min. For ErbB2 and ErbB3, antigenic retrieval was done via pressure cooking at 121°C for 5 min in Tris-EDTA buffer (pH 9.0). After quenching of endogenous peroxidase activity with 3% H_2O_2 for 10 min and blocking with bovine serum albumin for 30 min, sections were incubated at room temperature for 1 h with antibodies against EGFR at 1:50 dilution, ErbB2 at 1:5,000 dilution, ErbB3 at 1:100, ER at 1:50, phospho-AKT or phospho-ERK at 1:200 dilution. Detection was achieved with the Envision+/HRP system (Dakocytomation) or UltraVision HRP Polymer and DAB Plus Chromogen system (Lab Vision Corp.). For clinical samples in which the numbers were big and to achieve consistency, immunohistochemistry was done using the Dako Autostainer (Dakocytomation) with the conditions programmed as above. All slides were counterstained with Gill's hematoxylin for 1 min, dehydrated and mounted for light microscopic evaluation. Interpretation of H&E sections and analysis/scoring of immunohistochemistry data were all done by the same certified pathologist to maintain consistency.

Drug Assays

Cells (1.5×10^3) in 100 μL of complete medium were seeded in triplicate into 96-well flat-bottomed microtiter plates and allowed to equilibrate overnight at 37°C, 5% CO_2 before treatment with drugs. The final concentrations of drugs used were 0.5, 2, 8, and 32 μmol/L for Gefitinib. The drug was added to cells at 100 μL per well such that each well contained 0.02% of DMSO. The medium for the control cells also had a final DMSO concentration of 0.02% for comparison. Plates were incubated for 1, 24, 48, and 72 h at 37°C, 5% CO_2, prior to the addition of 20 μL of a 3-(4,5-dimethylthiazol-2-yl)-2,5-diphenyltetrazolium bromide reagent. The mixture was incubated at 37°C for 1 h, after which the absorbance was measured at 490 nm with reference to 655 nm.

Fluorescence *In situ* Hybridization

Fluorescence *in situ* hybridization (FISH) analysis of the *EGFR* gene was done following a standardized protocol. In brief, sections from tissues were mounted on Superfrost glass slides (Matsunami Glass Ind., Ltd., Japan), deparaffinized in xylene, and subsequently rehydrated. Pretreatment of slides was done according to the

manufacturer's instructions. A directly labeled mixture of LSI EGFR (Spectrum Orange) and CEP7 (Spectrum Green) probes (Vysis, Abbott) was used to evaluate the copy number of EGFR and CEP7, which is centromere on chromosome 7 for reference. For hybridization, the LSI EGFR/CEP 7 Dual-Color Probe was introduced onto the slide and protected by a Menzel microscope coverslip (22 × 22 mm), which was sealed with rubber cement. For denaturation, slides were heated to 85°C for 2 min and incubated overnight at 37°C in a humidified dark chamber. Afterwards, the rubber cement and the coverslip were removed. Finally, a drop of prolong antifade reagent (Invitrogen, Molecular Probes) was added onto a new coverslip and the slides were counterstained with 4,6-diamidino-2-phenylindole. Evaluation of signals was carried out using a motorized microscope (Olympus BX61) equipped with Spectral Imaging System (Applied Spectral Imaging) which contained FITC, TRITC and 4,6-diamidino-2-phenylindole filter set.

Results

iTRAQ-Based Phosphoproteomics Revealed Diminishing Tyrosine-Phosphorylated EGFR during Breast Cancer Progression

The cell lines in the MCF10AT model used in this study included MCF10A1, which is modeled after the normal epithelium; MCF10AT1K.cl2, MCF10CA1h, and MCF10CA1a.cl1, which is modeled after premalignant epithelium, low grade, and high grade lesions, respectively (20). They are abbreviated as A1, 1k, 1h, and 1a in this study. To prepare cells for phosphoproteomics analysis, cells were treated with pervanadate, a potent tyrosine phosphatase inhibitor, to enhance the presentation of tyrosine-phosphorylated proteins. The phosphoproteins were then affinity-captured using 4G10 antibodies, labeled with iTRAQ reagents (26) and analyzed using electrospray ionization-liquid chromatography tandem mass spectrometry to determine the relative phosphoprotein levels in the MCF10AT cells. The cells A1, 1k, 1h, and 1a were labeled with iTRAQ reagents 114, 115, 116, and 117, respectively. The ratios 115:114, 116:114, and 117:114 indicate the relative abundance of a potentially tyrosine-phosphorylated protein in 1k, 1h, and 1a with respect to A1. Our data showed that close to 50 proteins were differentially tyrosine phosphorylated. One of these was EGFR. As seen in Fig. 1A, the ratios of tyrosine-phosphorylated EGFR levels between 1k, 1h, and 1a referenced to A1 were progressively diminishing, suggesting loss of tyrosine-phosphorylated EGFR during disease progression. The data were of high statistical significance ($P < 0.05$). The tandem mass spectra of the three iTRAQ-labeled EGFR peptides detected and relatively quantified by electrospray ionization-mass spectrometry are shown in Fig. 1B. The EGFR protein was chosen for further studies for two reasons: (*a*) it is uncommon for receptor tyrosine kinases, which are oncogenes involved in many human cancers, to be lost in cancer cells, progressive loss of EGFR expression in breast cancer is therefore interesting; (*b*) the observation might have implications in the design of clinical trials involving EGFR inhibitors for breast cancer treatment. As the rest of the phosphoproteomics data also contained other novel findings of substantial nature, it is only appropriate to present them in a separate report.

Loss of EGFR Is An Early Event and Is Associated with Resistance to Gefitinib in Breast Cancer

In the experimental design described above involving the treatment of cells with pervanadate, differential phosphorylation of EGFR could be due to differential expression of EGFR or it could be due to differential tyrosine kinase or phosphatase activities that might arise from genetic aberrations. To determine which event is true, PV-stimulated MCF10AT cells were harvested and lysates immunoprecipitated with anti-EGFR antibodies. Two sets of immunoprecipitation were conducted. One set of immunoprecipitates was probed with antiphosphotyrosine antibodies to reveal the phosphorylation level of EGFR whereas another set was probed with anti-EGFR to show its expression level. As can be seen, the relative phosphorylation levels of EGFR protein across the MCF10AT cells were consistent with those revealed by the phosphoproteomics data (Fig. 2A, *top*). The data also showed a progressive loss of full-length EGFR, as indicated by its molecular weight, beginning with the early stage cancer cells (1h) with the later stage cancer cells (1a) expressing the least full-length EGFR (Fig. 2A, *bottom*). This showed that the differential phosphorylation of EGFR detected by the phosphoproteomics approach was due to the differential expression levels of EGFR. To determine whether the loss of EGFR expression was due to transcriptional or chromosomal aberrations, we conducted *FISH* analysis of *EGFR* on the cells. Out of 20 metaphases counted for each cell line, 50% of 1a cells had no signal whereas another 50% had only one signal/copy (Fig. 2B). 1k had normal *EGFR* gene copy number. This implied that the observed loss of EGFR was most likely a result of chromosomal anomaly. Although AT1k has normal gene copy normal (Fig. 2B), it is noteworthy that at steady state, the expression of EGFR protein in A1 was lower than 1k and 1h, whereas actin expression was the same across these cell lines (Fig. 2A). This could be due to the presence of aberrations such as deregulated modulation of EGFR in the cancer cell lines but this will not be investigated further because it is not our focus.

As EGFR is a target of Gefitinib and was observed to be lost in breast cancer, one would expect the response of late stage cancer cells to Gefitinib to be poorer than early stage cancer cells. To test this postulation, the various MCF10AT cell lines were treated with Gefitinib over a range of doses (0.5, 2, 8, and 32 μmol/L). Cell viability counts were determined daily using the 3-(4,5-dimethylthiazol-2-yl)-2,5-diphenyltetrazolium bromide assays over 3 days. Response herein is defined as ≥50% killing after 3 days of drug treatment. At AstraZeneca's recommended physiologic dose of ~0.5 μmol/L, the progression from 1k to 1a was marked by increasing resistance to Gefitinib, whereas the

A1 cells were most sensitive to Gefitinib (Fig. 2C). Although more killing was observed with higher doses, it might be due to random cytotoxicity rather than specific inhibition of EGFR by Gefitinib (data not shown). In the case of non–small cell lung cancer, *EGFR* mutation has been shown to confer sensitivity to Gefitinib. In the model used here, no EGFR mutation was observed in the entire kinase domain (exons 18–21; data not shown). In conclusion, loss of EGFR

A

Protein ID	No. of peptides	115:114	p-value 115:114	116:114	p-value 116:114	117:114	p-value 117:114
EGFR_human (P00533)	3	3.4133	1.28E-07	1.8410	1.53E-06	0.4885	1.66E-06

B

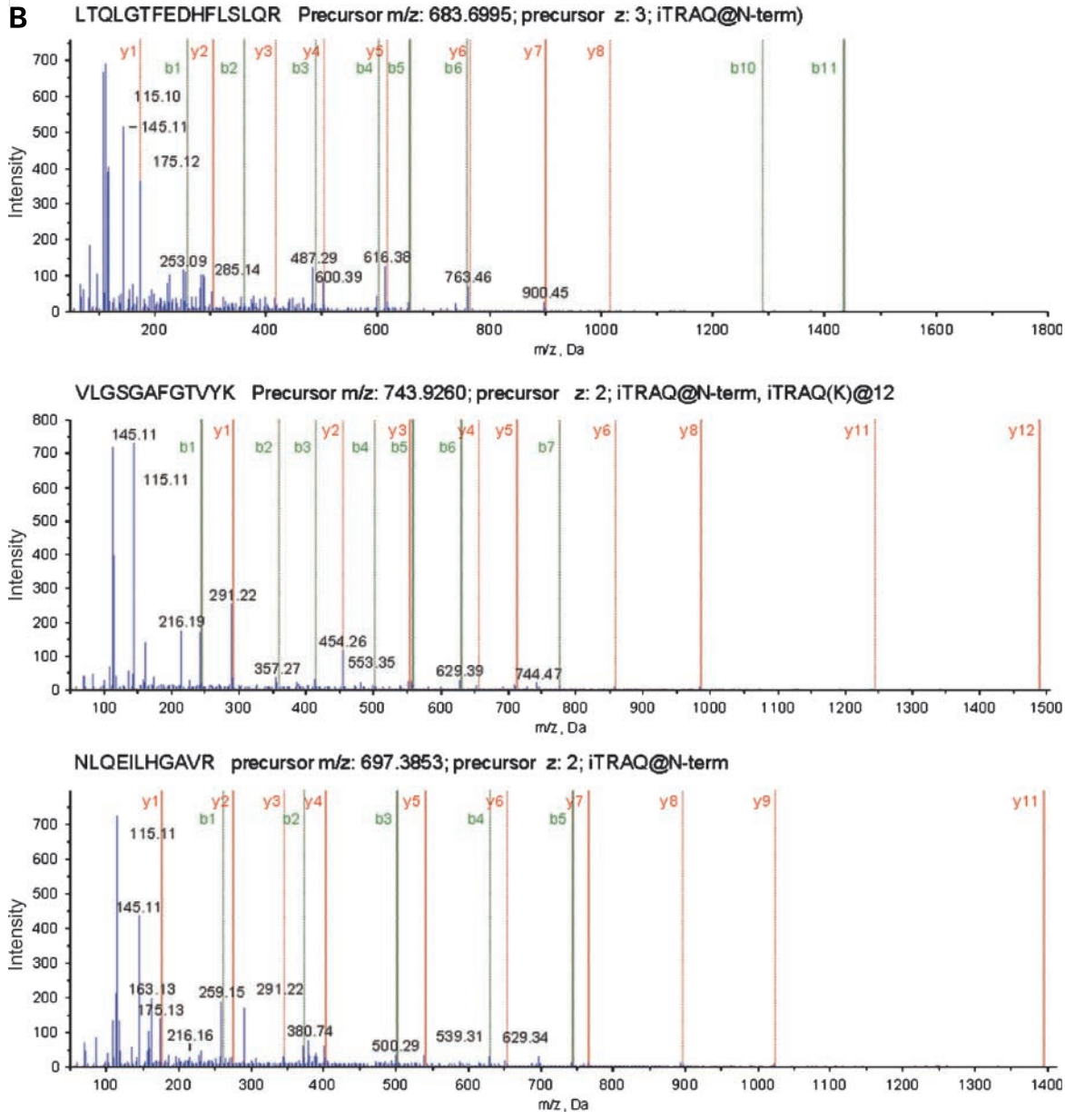

Figure 1. Phosphoproteomics of MCF10AT cells. Cells were stimulated with 1 mmol/L of pervanadate for 15 min and lysed. Lysates were subjected to affinity purification, labeled with iTRAQ reagents, and analyzed by liquid chromatography tandem mass spectrometry as detailed in Materials and Methods. A1, 1k, 1h, and 1a cells were labeled with 114, 115, 116, and 117 tags, respectively. **A,** the relative level of phosphorylated EGFR in 1k (115:114), 1h (116:114), and 1a (117:114) with respect to A1 cells as determined by electrospray ionization tandem mass spectrometry. All values are of high statistical significance. **B,** tandem mass spectra from three iTRAQ-labeled peptides of EGFR detected and relatively quantified using electrospray ionization tandem mass spectrometry.

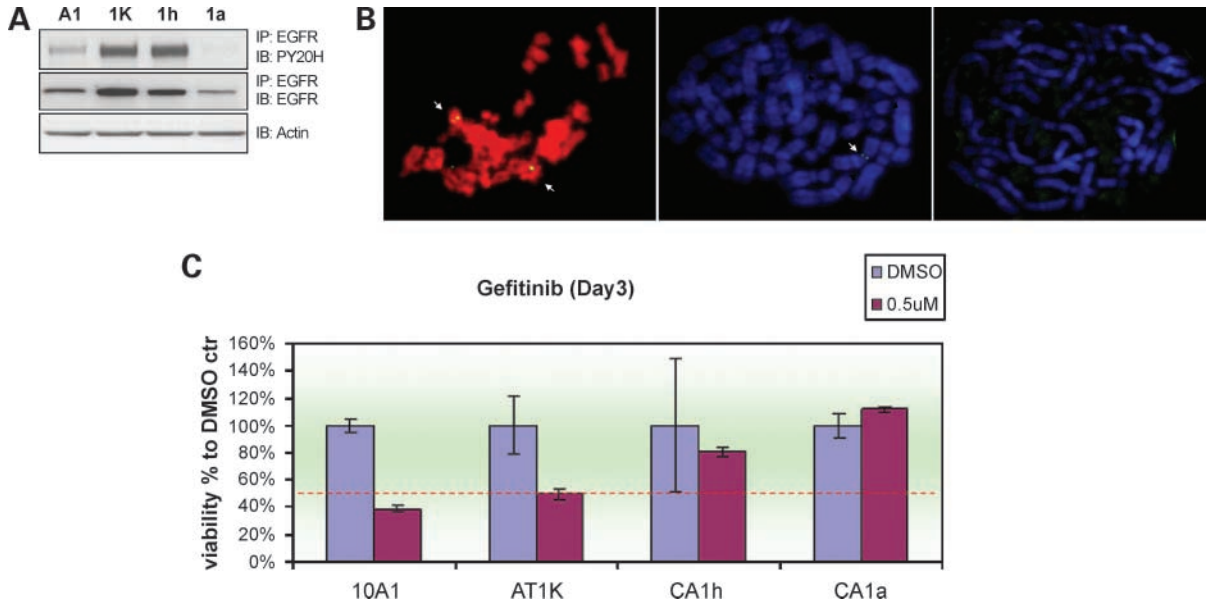

Figure 2. **A,** relative tyrosine phosphorylation and expression of EGFR in MCF10AT cells. A1, 1k, 1h, and 1a cells were grown in complete medium. When they reached 90% confluence, they were starved overnight and stimulated with pervanadate at 1 mmol/L for 15 min. They were then harvested and lysates were immunoprecipitated with anti-EGFR antibodies. One set of immunoprecipitates was probed with antiphosphotyrosine antibodies (*top*) whereas another was probed with anti-EGFR antibodies (*middle*). The whole cell lysates were also immunoblotted with antiactin to show normalization of protein amounts (*bottom*). **B,** FISH analysis of EGFR in 1k (*left*) and 1a cells (*middle* and *right*). 1k cells have two copies of EGFR (*arrows*). About 50% of 1a cells have one copy (*middle*) whereas the rest have no EGFR (*right*). **C,** response of MCF10AT cells to Gefitinib. After overnight culture, cells were treated with Gefitinib at various doses (0.5, 2, 8, and 32 μmol/L) and 3-(4,5-dimethylthiazol-2-yl)-2,5-diphenyltetrazolium bromide assays done daily over 3 d. Only the data for cells treated for 3 d with the manufacturer's recommended dose of 0.5 μmol/L are shown. Control cells that were grown in medium containing the same content of DMSO (0.02%; *blue columns*) as the treated cells but not treated with the respective drugs (*red columns*). *Red dotted line,* 50% cell viability.

occurring early during breast cancer progression was associated with resistance to Gefitinib although other molecular aberrations could also be responsible.

Constitutive Activation of PI3K and MAPK Pathways were Concomitant with Loss of EGFR Expression during Breast Cancer Progression

During the course of the study, there was no noticeable slowing down of cell growth and proliferation of 1h and 1a cancer cells despite the observed loss of EGFR compared with 1k cells. There are other derivative cell lines in the MCF10AT model that have different characteristics from those used in this study. Although the growth response of some of these cell lines with respect to EGF has been characterized (12), comparative studies of the signal transduction and cellular response to EGF across the four cell lines used in this study has never been reported. To study the influence of the loss of EGFR expression on EGF response, cells were either not treated or stimulated with 50 ng/mL of EGF for 3 days. Viability counts were measured daily using 3-(4,5-dimethylthiazol-2-yl)-2,5-diphenyltetrazolium bromide assays. Among the cancer cells, 1k was dependent on EGF for growth as reflected by the low proliferation rate in unstimulated cells compared with EGF-stimulated cells. In contrast, both 1h and 1a cells gained EGF-independent proliferation. Although 1h cells remained responsive to EGF, 1a cells had lost their responsiveness to EGF (Fig. 3A). Note that MCF10A normal mammary epithelial cells are well known to require other factors such as insulin, hydrocortisone, and cholera toxin in addition to EGF for growth. Next, we examined the proliferation rate of these cells *in vivo* by s.c. implanting them into the flanks of severe combined immunodeficiency mice and measuring the tumor volume at regular intervals. We observed that the time to tumor initiation and the rate of tumor growth were fastest for 1a (~3 weeks), followed by 1h and 1k (~2 months). A1 cells were not tumorigenic (Supplementary Fig. S1).[8] Taken together, the data suggest that, at least in this model system, EGFR expression is not critical for cell growth and proliferation in advanced cancer cells.

The finding that 1a cells had lost most of their EGFR but acquired EGF-independent growth suggested a gain of growth advantage through other mechanisms. Because MAPK and PI3K are major mitogenic pathways, we investigated whether these pathways could play a role in the MCF10AT system. Cells were either untreated or treated with 50 ng/mL of EGF over a time course. The lysates were first probed with antiphosphotyrosine antibodies to reveal

[8] Supplementary material for this article is available at Molecular Cancer Therapeutics Online (http://mct.aacrjournals.org/).

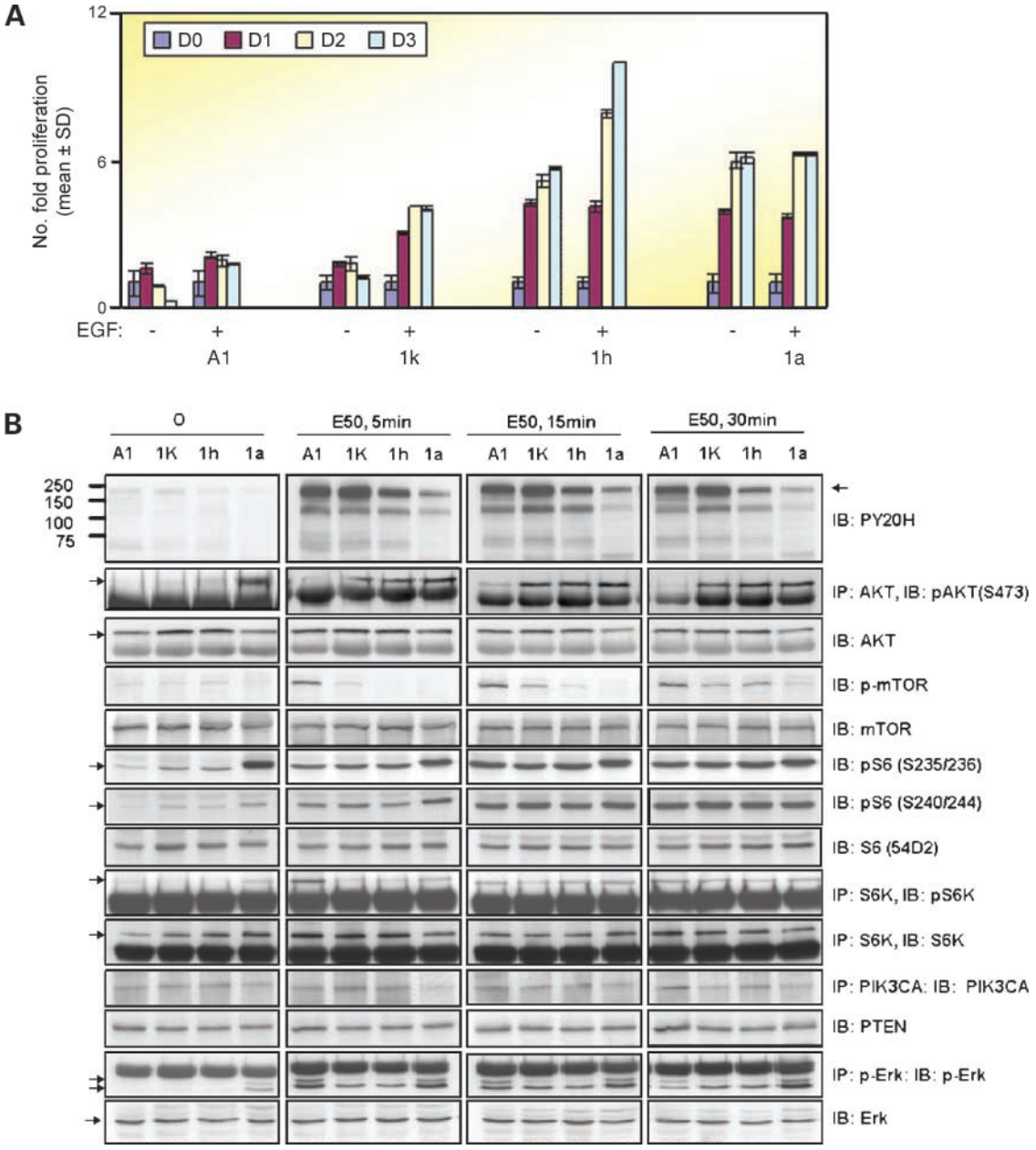

Figure 3. **A,** *in vitro* proliferation assays of MCF10AT cells in response to EGF. Serum-starved cells were either untreated or stimulated with EGF at 50 ng/mL and 3-(4,5-dimethylthiazol-2-yl)-2,5-diphenyltetrazolium bromide assay (Promega) done over 3 d. **B,** activation status of signaling pathways in MCF10AT cells in the absence or presence of EGF. Cells were either untreated or treated with EGF at 50 ng/mL for the indicated times and cell lysates were prepared. Neat lysates or immunoprecipitates were resolved by one-dimensional SDS-PAGE and immunoblotted with antiphosphotyrosine antibodies (*top*), protein-specific antibodies (AKT, mTOR, S6, S6K, PIK3CA, PTEN, and ERK) or phosphorylated protein – specific antibodies (p-AKT, p-mTOR, pERK, pS6, and pS6K).

the global tyrosine phosphorylation response of these cells. Consistent with the loss of EGFR expression observed in earlier section, the EGF-induced autophosphorylation of EGFR (indicated by an arrow) displayed a decreasing trend from 1k to 1a (Fig. 3B, *top*). Next, using a combination of immunoprecipitation and immunoblotting with protein-specific or phosphorylation site–specific antibodies, various signaling proteins in the PI3K/AKT and MAPK pathways were interrogated. These data are collectively presented in the rest of Fig. 3B. Constitutive phosphorylation of AKT (*panel 2*) and ribosomal S6 protein (*panels 6* and *7*) were strongest in 1a cells but were already present in 1h cells, albeit more weakly. Interestingly, the basal phosphorylation of mTOR, a downstream target of PI3K, was not apparently different in the various cell lines (*panel 4*). Rather, there seemed to

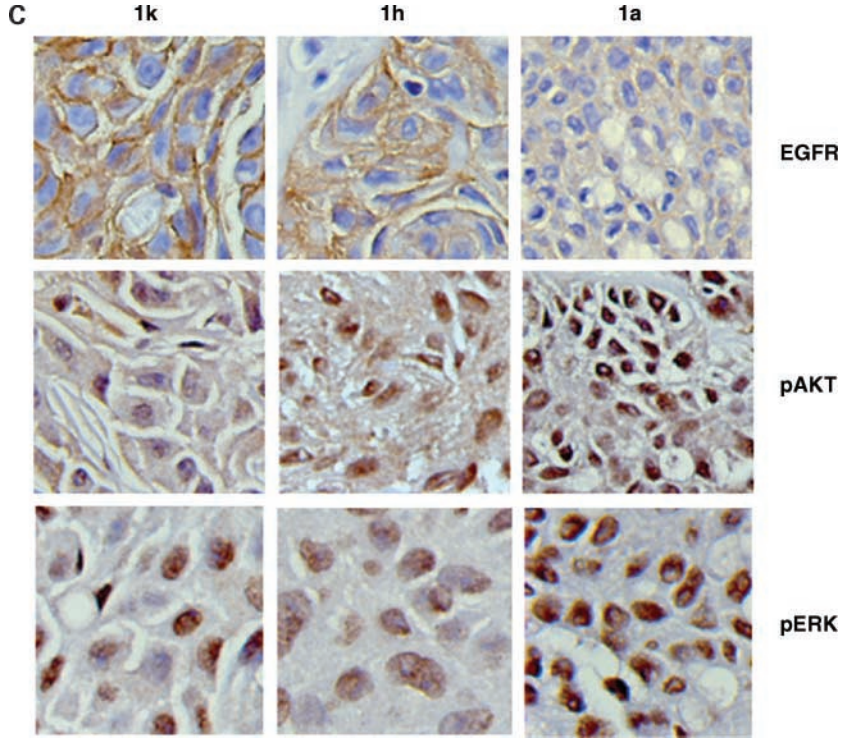

Figure 3 *Continued.* **C,** immunohistochemistry of EGFR (*top*), pAKT (*middle*), and pERK (*bottom*) on xenografted tumors from 1k, 1h, and 1a cells.

be a temporal delay in mTOR phosphorylation during disease progression in the following order: (fastest) A1 > 1k > 1h > 1a (slowest). *PIK3CA* mutation has recently been found in breast cancer (27). To investigate whether this was responsible for the constitutive activation of AKT pathway in the system used, we obtained pure cell clones and expanded them before sequencing exons 9 and 20, where hotspots mutation are known to occur in *PI3KCA*. The results revealed a heterozygous mutation at exon 20, A3140G (H1047R), known to confer activation to PIK3CA, the catalytic subunit of PI3K (28) only in 1h and 1a cells (Supplementary Fig. S2).[8] No other *PIK3CA* mutation at exons 9 and 20 were detected. Although activating *PIK3CA* mutation was present in 1h and 1a cells, constitutive activation of AKT/S6 pathway was stronger in 1a compared with 1h cells. Hence, we also investigated whether genetic aberrations of *PTEN*, a negative regulator of PI3K, could also be involved. Our results revealed that exons 5 to 8 of *PTEN* where hotspot mutations occur (29) were normal (data not shown). The expression levels of PTEN in these cells were also similar suggesting that it was not responsible for the differential basal activation of AKT/S6 in 1a and 1h. Although we have no concrete evidence, the heterogeneity of the population within individual cell lines may account for the differential levels of basal AKT/S6 activation. In other words, the 1a cell line may have a higher percentage of ''aberrant'' cells compared with 1h. Evidence for the presence of heterogeneity is provided by the observation seen in Fig. 2B in which 50% of the cell population had no *EGFR* gene, whereas 50% of them possessed one copy of *EGFR* allele.

Immunoblotting of phosphorylated ERK in these cells showed that constitutive ERK activation, as reflected by the presence of phosphorylated ERK in the nonstimulated state, was observed in 1a cells but not in other cells (panel 2 from the bottom). It is not clear at which point of the Ras/MAPK cascade could have contributed to this. To verify the key *in vitro* data in this section, we conducted the immunohistochemistry of EGFR, pAKT, and pERK on xenografted tumors. The results showed that the data from *in vitro* and animal model were in concordance (Fig. 3C). Altogether, the acquisition of ligand independent growth capability of 1h and 1a cells could be explained at least in part by constitutive activation of the PI3K/AKT and RAS/MAPK pathway although other aberrations are also likely (21).

Loss of EGFR as Reflected by MCF10AT Model Is Validated in Clinical Human Breast Cancers

A major limitation of using *in vitro* and even animal models is that frequently these systems lack the physiologic context present in the human body. To investigate whether the loss of EGFR expression observed in early cancer cells *in vitro* and in animal studies truly reflect the clinical settings, a total of 93 pairs of frozen, matched normal and breast tumor tissues of Asian origin were examined for EGFR expression via immunohistochemistry. The matched samples could be grouped into two categories. The first group (n = 59 pairs) consisted of matched normal tissues and tumors, which contained only a single type of lesion [infiltrative ductal carcinoma (IDC)]. A representative is shown in Fig. 4A (*top*). Here both the myoepithelial and ductal epithelial cells in the normal ducts were stained

positive for EGFR whereas the invasive epithelial components were devoid of EGFR. The second group (n = 34 pairs) consisted of matched normal tissues and tumors, which contained multiple lesions including hyperplasia, ductal carcinoma *in situ* (DCIS), and/or IDC. A representative is shown in Fig. 4A (*bottom*). Consistent with the above results, the normal tissue stained strongly for EGFR in both the myoepithelial and ductal epithelial cells. In the tumor section, the hyperplastic ductal cells displayed weaker than normal EGFR signal, which was completely lost in the DCIS and malignant ducts invading the stroma in the same section. A complete list of immunohistochemistry results with the bioclinical data are provided in Supplementary Table S1.[8] It should be highlighted that all immunohistochemistry assays were done using automated stainer to ensure consistency and reduce variability in staining procedures for accurate analysis. In summary, when matched normal and invasive carcinomas were compared, 92.8% (52 of 56) of the cases expressed more EGFR in the normal compared with tumor; 3.6% (2 of 56) showed the reverse trend; 1.8% (1 of 56) showed equal expression and 1.8% (1 of 56) showed negative expression in both samples (Table 1, *top*). Thirty-seven cases could not be determined due to lack of ductal cells in samples. When the expression of EGFR was compared among invasive carcinomas (IDC) alone, only 14.8% (13 of 88; five cases were not included for analysis because they lacked invasive cells) expressed detectable levels of EGFR (Table 1, *bottom*). This is a vast difference from normal breast where EGFR expression was detected in 95.2% (60 of 63) of the cases. Without normal samples for comparison, analysis of tumor samples alone, as is routinely done by many groups around the world, would have led to the erroneous interpretation that 18.4% of tumor cases analyzed ''overexpressed'' EGFR. All the above analyses were also done for ErbB2 (Table 1). ErbB2 is overexpressed in 64.2% (34 of 53) of the cases when matched normal and tumor samples were analyzed. In invasive carcinomas alone, ErbB2 expression could be detected (a score of +/− and above) in 77% (67 of 87) of the cases. If we define a score of 2+ or more as overexpression, then ErbB2 was overexpressed in 24% (21 of 87) of all cases. This is consistent with the 20% to 25% reported (30).

From the above data, the majority of the breast tumors either have no detectable or lesser EGFR expression compared with normal breast tissues. Hence, we proceeded to determine the statistical significance of the correlation between EGFR expression and tissue phenotypes—normal (N) and tumor (T); here we loosely define T as any lesion that was not normal, i.e., hyperplasia, carcinoma *in situ*, and infiltrative carcinoma because loss of EGFR could be detected in these lesions, albeit with different frequencies. To do this, immunohistochemistry-based EGFR expression data in Supplementary Table S1[8] was first scored (3+ = 3, 2+ = 2, 1+ = 1, +/− = 0; -ve = −1). Average values were taken for intermediate scores, e.g., 2+/1+ = 1.5. For grading with percentages, e.g., 2+ (10%), the score was given by the multiplication of the grade and percentage (2 × 0.1 = 0.2). Differences in EGFR expression between N and T samples were then calculated and paired-sample t tests were conducted. In some tumor cases that contained a spectrum of lesions, only EGFR expression value from the IDC component was used to represent tumor samples. In addition, some normal tissue sections have no epithelial components (fats only), whereas some tumor sections may contain normal epithelial cells. As a rule of thumb, EGFR expression values for normal samples were taken from the epithelial components in the normal sections, and where it was not possible, the value was then taken from the normal epithelial cells within tumor sections. From the analyses, we concluded that the EGFR expression in normal tissue was significantly different from that of tumor tissue ($P < 0.0001$; Table 2). The same was done to ErbB2 for comparison and although significant at $P = 0.008$, this is less significant than EGFR. To represent these statistical analyses visually, box plots for the distribution of EGFR and ErbB2 expressions in normal versus tumor samples were created and shown in Fig. 4B. It shows that lower EGFR and higher ErbB2 expressions were associated with breast tumor compared with normal tissues.

Loss of EGFR Occurred Early in a Major Subset of Asian Breast Cancers and Is Due to Loss of Gene Copy Number

The availability of a spectrum of lesions (hyperplasia to DCIS to invasive carcinomas) in 34 matched samples allowed us to investigate the relationship between EGFR expression and disease progression. As described above, EGFR expression was scored for each of the four categories of samples, i.e., normal (N), hyperplasia (HP), DCIS, and invasive carcinomas (IDC). In contrast to the analyses above, the readings for ''normal'' were taken from the normal epithelial components found within tumor samples for a closer reflection of progressive changes. Where no normal component was found in tumor samples, then the readings from matched sections taken from contralateral normal breasts would be used. In DCIS cases in which readings were available for myo- and ductal-epithelial cells, average values were taken. The relationships between EGFR expression and the various phenotypes were then examined using the ANOVA test, followed by the Tukey's HSD test as a post hoc to perform pair-wise comparisons to find out how EGFR distinguishes among the four groups. Polyserial correlation coefficients were also calculated for the correlation between differences in EGFR expression and disease progression. Significant results were obtained for both analyses. The ANOVA test followed by Tukey's HSD test revealed that normal and hyperplastic lesions could be clustered as one group, whereas DCIS and IDC could be clustered as another group ($P < 0.001$; Fig. 5A, *top*). In addition, we obtained a correlation coefficient of −0.371 using a polyserial correlation analysis ($P = 0.024$; Table 2). Together with the box plot analysis (Fig. 5A, *bottom*), these data revealed statistically significant progressive loss of EGFR expression during breast cancer development, and that early and late lesions could be discriminated by EGFR expression levels.

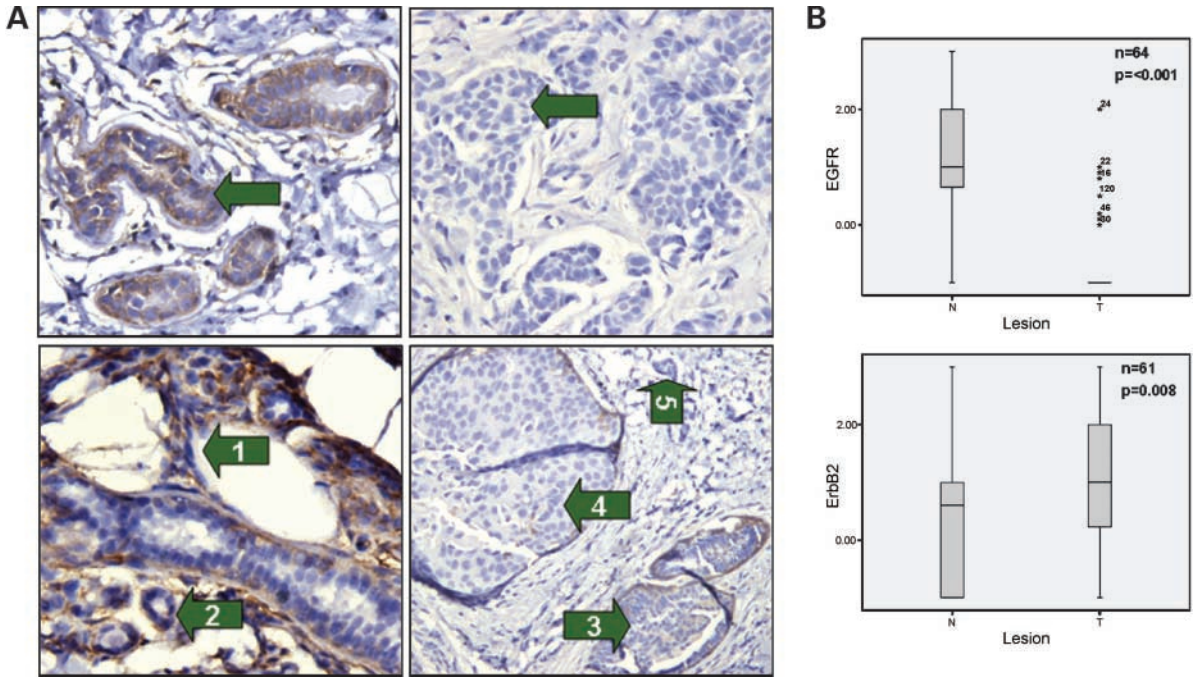

Figure 4. **A,** immunohistochemistry of EGFR in clinical breast samples. *Top,* EGFR expression in matched normal and tumor breast samples from patient 255. The tumor from this patient showed only a single type of lesion: invasive carcinoma. *Arrows,* positive EGFR stain in normal duct (*left*); invasive tumor cells showing the absence of EGFR signals (*right*). *Bottom,* EGFR expression in matched normal and tumor breast samples from patient 813. The tumor of this patient contained a spectrum of lesions. *Arrow 1,* duct with mild epithelial hyperplasia; *arrow 2,* normal duct; both showed positive staining; *arrow 3,* weak positive EGFR stain in ducts with epithelial hyperplasia; *arrow 4,* negative EGFR stains in epithelial cells from DCIS; and *arrow 5,* malignant duct invading the stroma. **B,** box plots of the distribution of EGFR (*left*) and ErbB2 (*right*) expressions in normal versus tumor samples. *, extreme values (cases with values more than three box lengths from either the upper or lower edge of the box).

There was no strong significant correlation between ErbB2 expression with disease progression. The *P* value for ANOVA analysis is 0.328 and although polyserial correlation gave a significant *P* value of 0.031, the model is not really a very good fit as another statistical calculation done in conjunction with the polyserial correlation indicated that the underlying assumption of bivariate normality is not well fulfilled. Thus, the test is

Table 1. Summary of EGFR expression in clinical breast samples and clinical-pathology data

Type of lesion	EGFR expression		ErbB2 expression	
	Trend	Frequency (%)	Trend	Frequency (%)
Normal and IDC only	*N* > IDC	52/56; 92.8%	*N* > IDC	16/53; 30.2%
	N < IDC	2/56; 3.6%	*N* < IDC	34/53; 64.2%
	N = IDC (positive)	1/56; 1.8%	*N* = IDC (positive)	2/53; 3.8%
	N = IDC (negative)	1/56; 1.8%	*N* = IDC (negative)	1/53; 1.9%
Type of lesion	Positive EGFR expression		Positive ErbB2 expression	
	Frequency (%)		Frequency (%)	
Normal	60/63; 95.2%		40/57; 70.2%	
Hyperplasia	7/12; 58.3%		8/11; 72.7%	
DCIS	11/28; 39.3%		14/22; 63.6%	
IDC	13/88; 14.8%		67/87; 77.0%	

NOTE: Positive expression is defined as an immunohistochemistry score of +/− and above, so long as it has a stronger signal than negative expression.

Table 2. Statistical analyses of the relationships between different factors using experimental and clinical data from normal and tumor samples

Factors	*P*	Methods	Coefficient	Sample size	
EGFR expression versus types of lesion (normal and tumor)	<0.001	Paired *t* test	—	64 pairs	
ErbB2 expression versus types of lesion (normal and tumor)	0.008	Paired *t* test	—	61 pairs	
EGFR expression versus disease progression	<0.001	ANOVA	—	81 pairs	Group N, 20; HP, 4; DCIS, 14; IDC, 22
	<0.001	Polyserial correlation	0.371		

NOTE: Only significant data ($P < 0.05$) are shown. For a full list of analyses, please see Supplementary Table S2.[8]

less powerful (Supplementary Table S2).[8] We have also conducted a considerable number of other correlational analyses between the differences in EGFR expression (between normal and tumor) with other clinical variables such as disease-free survival, overall survival, nodal status, tumor diameter, and ER status. A bigger difference in EGFR expression between normal and tumor samples seems to correlate better with nodal status (i.e., metastasis) compared with a smaller difference. This was very close to 95% confidence and may have an implication for predicting metastasis pending larger cohort studies ($P = 0.065$; Supplementary Table S2).[8]

Finally, we conducted FISH analysis on the clinical samples to investigate whether the underlying cause for the decrease in EGFR expression in breast tumors could be due to allelic loss. Immunohistochemical analyses have been done extensively on all available cases and confirmed the decrease of EGFR expression at the protein level. As FISH analysis was employed only as a means to explore the possibility of allelic loss as a contributing factor for the latter, only a total of five matched normal and tumor samples were used. The samples chosen contained a spectrum of lesions including DCIS and IDC. For each of these lesions (normal, DCIS, and IDC), between 100 and 200 nuclei were scored for signals from both CEP7 and *EGFR* DNA probes. In other words, more than 500 nuclei were counted per group. Only signals from nonoverlapping nuclei were included in the analysis. Two signals of the same size in close proximity, not connected by a link, were counted as two signals. A diffuse signal was regarded as one signal if it was contiguous and within an acceptable boundary. Two small signals connected by a visible link were counted as one signal. Due to molecular heterogeneity of samples and other standard technical challenges posed to the analysis (e.g., overlapping nuclei, interference from fatty tissues in normal breast, etc.), the number of EGFR and CEP7 gene copy numbers were determined for each of the five normal, DCIS, and IDC lesions and were expressed as an average ratio of *EGFR*/CEP7. Standard deviation was then calculated (Supplementary Table S3)[8] and values plotted (Fig. 5B). Cells from matched normal samples had a ratio of close to 1 reflecting normal gene copy numbers. Note that this value is not exactly 1.0 and could be due to technical reasons and/or the presence of a mild degree of genetic aberration even in the normal tissue. On the other hand, DCIS and IDC samples had ratios of ~0.6, implying loss of *EGFR* allele. This is consistent with the immunohistochemistry data that loss of EGFR could be detected as early as the preneoplastic lesion (DCIS). However, the loss of EGFR signals from immunohistochemistry data was more drastic than that revealed by FISH and this could be explained by the possibility that positive signals from FISH do not necessarily reflect a full-length allele, whereas due to the antibodies selected for immunohistochemistry, only full-length EGFR proteins were detected. As representatives, the FISH images of the nuclei of cells from IDC samples from various patients analyzed are shown in Fig. 5C. The figure shows that the molecular heterogeneity of *EGFR* copy number (and even chromosome 7) in breast tumor cells. Some revealed loss of one or both copies of *EGFR* whereas others displayed multiple signals of *EGFR* and CEP7. A higher resolution molecular analysis of *EGFR* alleles would be needed to further comprehend the complexity associated with this ''oncogene''.

Discussion

Our study shows that progression from low-grade cancer to high-grade cancer is marked by down-regulation of EGFR expression. This observation was first made in the MCF10AT model and was subsequently validated in human clinical samples supporting the notion that the *in vitro* MCF10AT model is able to mirror molecular events in the clinical setting. Although the diminution of EGFR expression in advanced cancer is not clear, gaining independence from growth factor might provide survival advantage for solid tumors. In addition, excessively strong EGFR signaling might be antagonistic on cancer cell survival in some cases (31). An interesting parallel is seen in the case of *Runx3*, a tumor suppressor gene. Its expression has been reported to be down-regulated in gastric cancer but overexpressed in basal cell carcinoma (32). These data point to an increasingly observed

phenomenon of proteins having both tumor suppressor and oncogene roles, the nature of which may be dependent on the stoichiometry of the proteins or other variables in the biological condition studied. On the other hand, ERBB2 and ERBB3 expression, as assayed by immunoblotting and immunohistochemistry, were maintained in the cancer cell lines used in this study (Supplementary Fig. S3),[8] suggesting the critical role of these receptors throughout the entire progression of the disease.

Analysis of clinical samples revealed that ~93% of the matched cases expressed more EGFR in normal compared with tumor samples, indicating loss of EGFR during breast cancer progression. FISH analysis done on clinical samples revealed that on average, both DCIS and IDC lesions have ~26% to 28% less *EGFR* gene copy numbers compared with normal cells. This is novel because until now, there has been no evidence of EGFR alterations at the chromosomal level in breast cancer (11), although it is noteworthy that loss of *EGFR* copy number has been detected in colorectal cancer (33). Our data questioned the validity of the numerous claims of EGFR overexpression in breast cancer. Besides, amplification of *EGFR* gene, if any, is infrequent in breast cancer (34). Our observation of the loss of EGFR in breast tumor agrees with previous work that reported lower EGFR expression in tumors compared with benign lesions (35–38). However, these authors did not use matched normal samples for comparison, and the study design was flawed by the diverse genetic backgrounds of the samples used which could have blunted

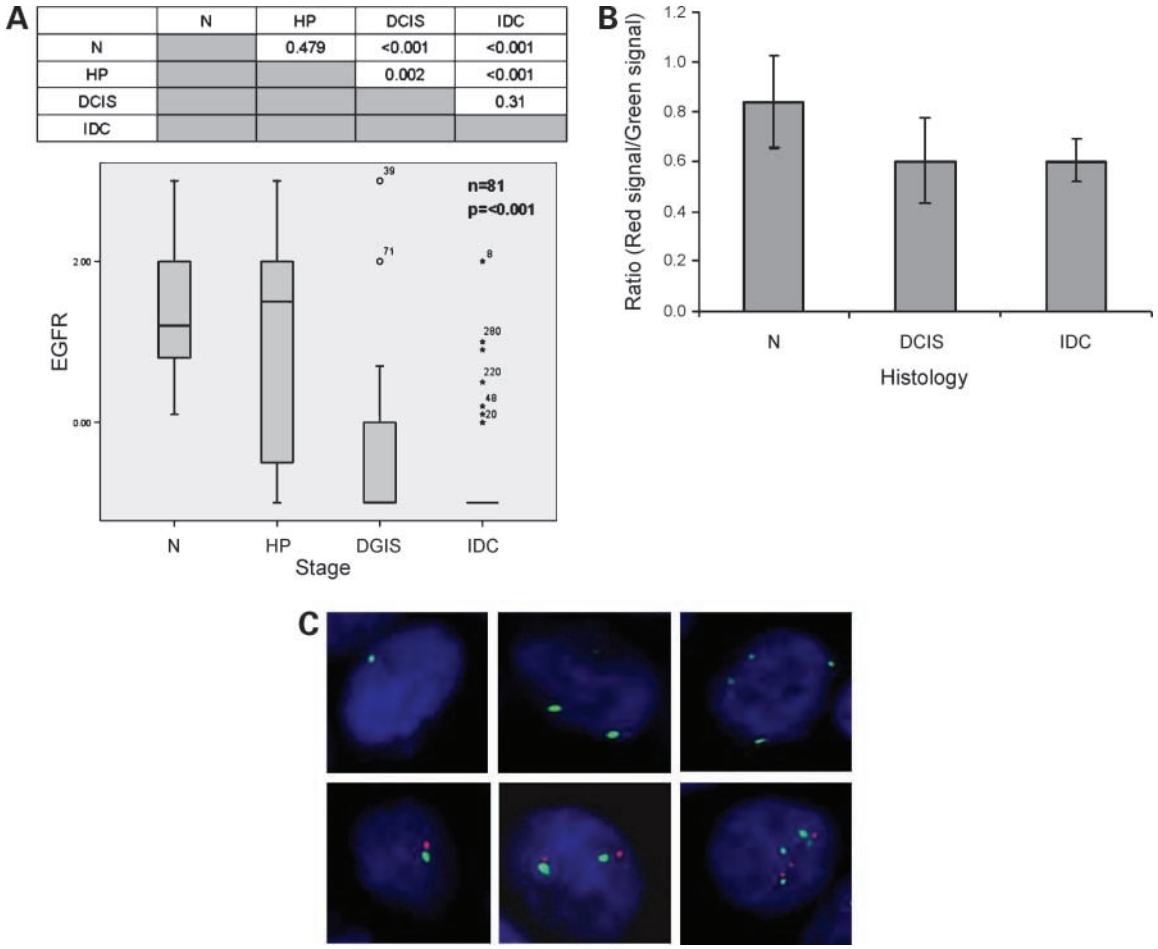

Figure 5. **A,** EGFR expression and disease progression. *Top, P* values obtained from Tukey's HSD test (as post hoc for ANOVA) for pairwise comparison of the groups. A value of <0.05 indicates that there was a significant difference in the mean value of the differences in EGFR expression between the two groups, i.e., difference in EGFR expression could discriminate between the two groups. The reverse is true. *Bottom,* box-plot for difference in EGFR expression for the four groups (N, HP, DCIS, and IDC). The box length is equivalent to the interquartile range whereas the ''whiskers'' are the minimum and maximum values (excluding outlier and extremes). *, extreme values (cases with values more than three box lengths from either the upper or lower edge of the box). ○, outliers (cases with values between one and a half and three box lengths from the upper or lower edge of the box). **B,** FISH analysis of EGFR in five sets of matched clinical breast samples. The number of green (CEP7) and red (EGFR) signals were obtained from nonoverlapping nuclei from normal, DCIS and IDC lesions from five matched normal and tumor samples. The average ratio of EGFR/CEP7 gene copy number was then obtained, SD was calculated (Supplementary Table S3),[8] and values plotted on bar charts. **C,** FISH images of cancer cells from IDC samples of various patients analyzed showing molecular heterogeneity associated with EGFR and CEP7 gene copy number.

their analyses. In contrast, our study not only employed matched samples, we also included a developmental dimension to EGFR expression during disease progression using tumor samples that contained a spectrum of lesions, i.e., hyperplasia, DCIS, and invasive ductal carcinomas. This allowed us to track EGFR expression changes more meaningfully during progression. In this study, we presented novel evidence of the progressive loss of EGFR expression in breast cancer and that diminution of EGFR expression could be detected early in preneoplastic lesions such as DCIS with high statistical confidence. This is fully supported by data from analyses of *in vitro*, xenograft, and clinical samples. EGFR expression status did not show any prognostic value in our current study and is consistent with another report (39).

When the status of EGFR expression was analyzed in IDC-only samples, we observed positive expression in ~15% of the cases. This is consistent with some studies that reported around the low 20% in the 2000s (40, 41) and is in contrast to others that reported a higher frequency of between 40% and 50% in the early 1990s (6, 42). Similarly, whereas there have been a couple of reports that supported the inverse relationship of ER and EGFR expression status, no statistically significant relationship between these two proteins was observed in our study (8, 39). Modern techniques, study design, and epidemiologic differences might account for the apparent discrepancies. Technically, the choice of antibodies is critical in immunohistochemistry (43). Before we conducted full-scale analysis, we screened various antigen retrieval methods and four kinds of EGFR antibodies from different sources (Abcam, Cell Signaling Technology, Becton Dickinson, and Dakocytomation)—two against the intracellular region (Cell Signaling Technology and Becton Dickinson) and two against the extracellular region of EGFR (Abcam and Dakocytomation) on a limited set of samples. The objective was to select an antibody that could detect EGFR at the plasma membrane, where most EGFR reside. This is to ensure that only the full-length and functional EGFR was examined. In summary, we found that only the DAKO antibodies directed against the extracellular region of EGFR used in conjunction with its antigen retrieval kit (modified citrate buffer; pH 6.1) satisfied this criterion. The DAKO antibodies have also been shown to detect full-length EGFR in Western blots (Supplementary Fig. S4).[8] The other sources of antibodies either gave a cytosolic presentation or extremely weak overall signal. Another technical consideration is the choice of sample processing method. Here, we used only freshly prepared paraffin-embedded blocks from frozen tissues requested from tissue repositories. Using the conditions that we optimized as described above, we found that immunohistochemistry of EGFR with most of archival paraffin-embedded blocks from local pathology labs did not give detectable EGFR signals in both normal and tumor samples. We found this to be unusual, and led us to the notion that the antigenic sites could have been ''destroyed'' during prolonged storage (44). In contrast, sections of freshly embedded normal tissues frequently gave unambiguous EGFR signals. In the case of study design, patient selection is likely to influence the outcome(s) of the study drastically. For example, the work by Tsutuis et al. used samples from patients with recurrent breast cancer, whereas no such prior selection was applied before analyses. The influence of epidemiologic differences, which explains the increasing importance of individualized medicine on any study, is supported by many pharmacogenomic reports, including the fact that *EGFR* mutation in non–small cell lung cancer has been observed in much higher frequency in Asian population than in Western continents (45).

In the clinical setting, not all cases of DCIS progress to carcinoma and whether all patients with DCIS should receive radiotherapy (or chemotherapy) after breast-conserving surgery remains a topic of active debate (46). Despite the relatively small data set, our study generated a testable hypothesis in which loss of EGFR expression could aid in determining the risk of DCIS developing into invasive carcinoma and could therefore help select patients for adjuvant therapy. Loss of EGFR expression and maintenance of ErbB2 and ErbB3 expression were observed in the MCF10AT model system. Although we do not have immunohistochemical data for ErbB3 for the clinical samples, our *in vitro* data implied that it is probably present throughout disease progression. Interestingly, like the EGFR reported here, expression of ErbB4 is uncommon in breast cancer and ErbB4 expression may be suppressed in carcinoma (47, 48). Taken together, there may be a radical shift towards the reliance of cancer cells on ErbB2/ErbB3 signaling during progression. These observations might explain the poor outcomes of clinical trials of Gefitinib on breast cancer for at least some advanced populations of breast cancer and the relatively better outcomes achieved with anti-ErbB2 therapy such as Herceptin. A more successful use of Gefitinib for breast cancer treatment may be restricted to early cancer, where EGFR is present, in combination with chemotherapy and will probably benefit from patient selection via EGFR expression screening. Perhaps, more importantly, drugs targeting both ErbB2 and ErbB3, despite the latter having no intrinsic kinase activity, might be potentially useful for early and/or late stage breast cancer. For example, the use of Pertuzumab/Omnitarg, which blocks ErbB2 dimerization with other EGFR members might benefit by targeting patients who are ErbB3-positive and have low/high ErbB2 protein rather than by selecting patients based on ErbB2 expression alone. Obviously, the presence of other molecular aberrations like those reported in this study, e.g., *PIK3CA* mutation is likely to present further challenges to therapeutic strategies.

As we advance into an era of individualized medicine, the design of clinical trials will similarly need to consider the molecular heterogeneity of disease. We hope that this study would provide at least some basis for the design of clinical trials involving tyrosine kinase inhibitors against the EGFR family members.

Acknowledgments

We thank Professors Saraswati Sukumar at the Sidney Kimmel Comprehensive Cancer Center, Richard J. Epstein at the Hong Kong University, and Graeme Guy at the Institute of Molecular and Cell Biology, Singapore, for scientific advice and critical reading of the manuscript. We also thank Dr. Jianbiao Zhou, Dr. Richie Soong, Xiaohui Liang, and Leong See Hon (under Prof. Kon Oi Lian) for technical support.

References

1. Manning G, Whyte DB, Martinez R, Hunter T, Sudarsanam S. The protein kinase complement of the human genome. Science 2002;298: 1912 – 34.

2. Robinson DR, Wu YM, Lin SF. The protein tyrosine kinase family of the human genome. Oncogene 2000;19:5548 – 57.

3. Blume-Jensen P, Hunter T. Oncogenic kinase signalling. Nature 2001; 411:355 – 65.

4. Lim YP. Mining the tumor phosphoproteome for cancer markers. Clin Cancer Res 2005;11:3163 – 9.

5. Biscardi JS, Ishizawar RC, Silva CM, Parsons SJ. Tyrosine kinase signalling in breast cancer: epidermal growth factor receptor and c-Src interactions in breast cancer. Breast Cancer Res 2000;2:203 – 10.

6. Klijn JG, Berns PM, Schmitz PI, Foekens JA. The clinical significance of epidermal growth factor receptor (EGF-R) in human breast cancer: a review on 5232 patients. Endocr Rev 1992;13:3 – 17.

7. Tsutsui S, Ohno S, Murakami S, Hachitanda Y, Oda S. Prognostic value of epidermal growth factor receptor (EGFR) and its relationship to the estrogen receptor status in 1029 patients with breast cancer. Breast Cancer Res Treat 2002;71:67 – 75.

8. Ferrero JM, Ramaioli A, Largillier R, et al. Epidermal growth factor receptor expression in 780 breast cancer patients: a reappraisal of the prognostic value based on an eight-year median follow-up. Ann Oncol 2001;12:841 – 6.

9. Rampaul RS, Pinder SE, Wencyk PM, et al. Epidermal growth factor receptor status in operable invasive breast cancer: is it of any prognostic value? Clin Cancer Res 2004;10:2578.

10. Barlesi F, Tchouhadjian C, Doddoli C, et al. Gefitinib (ZD1839, Iressa) in non-small-cell lung cancer: a review of clinical trials from a daily practice perspective. Fundam Clin Pharmacol 2005;19:385 – 93.

11. Arteaga CL, Truica CI. Challenges in the development of anti-epidermal growth factor receptor therapies in breast cancer. Semin Oncol 2004;31:3 – 8.

12. Miller FR. Xenograft models of premalignant breast disease. J Mammary Gland Biol Neoplasia 2000;5:379 – 91.

13. Santner SJ, Dawson PJ, Tait L, et al. Malignant MCF10CA1 cell lines derived from premalignant human breast epithelial MCF10AT cells. Breast Cancer Res Treat 2001;65:101 – 10.

14. Malaney S, Daly RJ. The ras signaling pathway in mammary tumorigenesis and metastasis. J Mammary Gland Biol Neoplasia 2001;6: 101 – 13.

15. Chong BE, Hamler RL, Lubman DM, Ethier SP, Rosenspire AJ, Miller FR. Differential screening and mass mapping of proteins from premalignant and cancer cell lines using nonporous reversed-phase HPLC coupled with mass spectrometric analysis. Anal Chem 2001;73: 1219 – 27.

16. Chong BE, Lubman DM, Miller FR, Rosenspire AJ. Rapid screening of protein profiles of human breast cancer cell lines using non-porous reversed-phase high performance liquid chromatography separation with matrix-assisted laser desorption/ionization time-of-flight mass spectral analysis. Rapid Commun Mass Spectrom 1999;13:1808 – 12.

17. Chong BE, Lubman DM, Rosenspire A, Miller F. Protein profiles and identification of high performance liquid chromatography isolated proteins of cancer cell lines using matrix-assisted laser desorption/ionization time-of-flight mass spectrometry. Rapid Commun Mass Spectrom 1998;12: 1986 – 93.

18. Starcevic SL, Diotte NM, Zukowski KL, Cameron MJ, Novak RF. Oxidative DNA damage and repair in a cell lineage model of human proliferative breast disease (PBD). Toxicol Sci 2003;75:74 – 81.

19. Starcevic SL, Elferink C, Novak RF. Progressive resistance to apoptosis in a cell lineage model of human proliferative breast disease. J Natl Cancer Inst 2001;93:776 – 82.

20. Tang B, Vu M, Booker T, et al. TGF-β switches from tumor suppressor to prometastatic factor in a model of breast cancer progression. J Clin Invest 2003;112:1116 – 24.

21. Worsham MJ, Pals G, Schouten JP, et al. High-resolution mapping of molecular events associated with immortalization, transformation, and progression to breast cancer in the MCF10 model. Breast Cancer Res Treat 2006;96:177 – 86.

22. Chen Y, Low TY, Choong LY, et al. Phosphoproteomics identified Endofin, DCBLD2 and KIAA0582 as novel targets of EGF signaling and Gefitinib in human cancer cells. Proteomics 2007;7:2384 – 97.

23. Lim YP, Diong LS, Qi R, Druker BJ, Epstein RJ. Phosphoproteomic fingerprinting of epidermal growth factor signaling and anti-cancer drug action in human tumor cells. Mol Cancer Ther 2003;2: 1369 – 77.

24. Lim YP, Wong CY, Ooi LL, Druker BJ, Epstein RJ. Selective tyrosine hyperphosphorylation of cytoskeletal and stress proteins in primary human breast cancers: implications for adjuvant use of kinase-inhibitory drugs. Clin Cancer Res 2004;10:3980 – 7.

25. Lim YP, Low BC, Lim J, Wong ES, Guy GR. Association of atypical protein kinase C isotypes with the docker protein FRS2 in fibroblast growth factor signaling. J Biol Chem 1999;274:19025 – 34.

26. Ross PL, Huang YN, Marchese JN, et al. Multiplexed protein quantitation in *Saccharomyces cerevisiae* using amine-reactive isobaric tagging reagents. Mol Cell Proteomics 2004;3:1154 – 69.

27. Samuels Y, Wang Z, Bardelli A, et al. High frequency of mutations of the PIK3CA gene in human cancers. Science 2004;304:554.

28. Kang S, Bader AG, Vogt PK. Phosphatidylinositol 3-kinase mutations identified in human cancer are oncogenic. Proc Natl Acad Sci U S A 2005; 102:802 – 7.

29. Bonneau D, Longy M. Mutations of the human PTEN gene. Hum Mutat 2000;16:109 – 22.

30. Hayes DF, Thor AD. c-erbB-2 in breast cancer: development of a clinically useful marker. Semin Oncol 2002;29:231 – 45.

31. Smida Rezgui S, Honore S, Rognoni JB, Martin PM, Penel C. Up-regulation of α2β1 integrin cell-surface expression protects A431 cells from epidermal growth factor-induced apoptosis. Int J Cancer 2000;87: 360 – 7.

32. Salto-Tellez M, Peh BK, Ito K, et al. RUNX3 protein is overexpressed in human basal cell carcinomas. Oncogene 2006;25:7646 – 9.

33. Sauer T, Guren MG, Noren T, Dueland S. Demonstration of EGFR gene copy loss in colorectal carcinomas by fluorescence *in situ* hybridization (FISH): a surrogate marker for sensitivity to specific anti-EGFR therapy? Histopathology 2005;47:560 – 4.

34. Umemura S, Takekoshi S, Suzuki Y, Saitoh Y, Tokuda Y, Osamura RY. Estrogen receptor-negative and human epidermal growth factor receptor 2-negative breast cancer tissue have the highest Ki-67 labeling index and EGFR expression: gene amplification does not contribute to EGFR expression. Oncol Rep 2005;14:337 – 43.

35. Dittadi R, Donisi PM, Brazzale A, Cappellozza L, Bruscagnin G, Gion M. Epidermal growth factor receptor in breast cancer. Comparison with non malignant breast tissue. Br J Cancer 1993;67:7 – 9.

36. Moller P, Mechtersheimer G, Kaufmann M, et al. Expression of epidermal growth factor receptor in benign and malignant primary tumours of the breast. Virchows Arch A Pathol Anat Histopathol 1989; 414:157 – 64.

37. Tauchi K, Hori S, Itoh H, Osamura RY, Tokuda Y, Tajima T. Immunohistochemical studies on oncogene products (c-erbB-2, EGFR, c-myc) and estrogen receptor in benign and malignant breast lesions. With special reference to their prognostic significance in carcinoma. Virchows Arch A Pathol Anat Histopathol 1989;416:65 – 73.

38. Tsutsumi Y, Naber SP, DeLellis RA, et al. neu oncogene protein and epidermal growth factor receptor are independently expressed in benign and malignant breast tissues. Hum Pathol 1990;21:750 – 8.

39. Tsutsui S, Kataoka A, Ohno S, Murakami S, Kinoshita J, Hachitanda Y. Prognostic and predictive value of epidermal growth factor receptor in recurrent breast cancer. Clin Cancer Res 2002;8:3454 – 60.

40. Abd El-Rehim DM, Pinder SE, Paish CE, et al. Expression and co-expression of the members of the epidermal growth factor receptor (EGFR) family in invasive breast carcinoma. Br J Cancer 2004;91:1532 – 42.

41. Park K, Han S, Shin E, Kim HJ, Kim JY. EGFR gene and protein expression in breast cancers. Eur J Surg Oncol 2007;33:956 – 60.

42. Fox SB, Smith K, Hollyer J, Greenall M, Hastrich D, Harris AL. The epidermal growth factor receptor as a prognostic marker: results of 370 patients and review of 3009 patients. Breast Cancer Res Treat 1994;29: 41 – 9.

43. Press MF, Hung G, Godolphin W, Slamon DJ. Sensitivity of HER-2/neu antibodies in archival tissue samples: potential source of error in immunohistochemical studies of oncogene expression. Cancer Res 1994; 54:2771 – 7.

44. Fergenbaum JH, Garcia-Closas M, Hewitt SM, Lissowska J, Sakoda LC, Sherman ME. Loss of antigenicity in stored sections of breast cancer tissue microarrays. Cancer Epidemiol Biomarkers Prev 2004;13:667 – 72.

45. Calvo E, Baselga J. Ethnic differences in response to epidermal growth factor receptor tyrosine kinase inhibitors. J Clin Oncol 2006;24: 2158 – 63.

46. Silverstein MJ, Buchanan C. Ductal carcinoma *in situ*: USC/Van Nuys prognostic index and the impact of margin status. Breast 2003;12: 457 – 71.

47. Srinivasan R, Poulsom R, Hurst HC, Gullick WJ. Expression of the c-erbB-4/HER4 protein and mRNA in normal human fetal and adult tissues and in a survey of nine solid tumour types. J Pathol 1998;185: 236 – 45.

48. Vogt U, Bielawski K, Schlotter CM, Bosse U, Falkiewicz B, Podhajska AJ. Amplification of erbB-4 oncogene occurs less frequently than that of erbB-2 in primary human breast cancer. Gene 1998;223:375 – 80.